International Journal of Architectural, Civil and Construction Sciences
ISSN: 2415-1734
Vol:3, No:10, 2009

Stochastic Subspace Modelling of Turbulence

M.T.Sichani, B.J.Pedersen, S.R.K.Nielsen

Abstract—Turbulence of the incoming wind field is of paramount importance to the dynamic response of civil engineering structures. Hence reliable stochastic models of the turbulence should be available from which time series can be generated for dynamic response and structural safety analysis. In the paper an empirical cross spectral density function for the along-wind turbulence component over the wind field area is taken as the starting point. The spectrum is spatially discretized in terms of a Hermitian cross-spectral density matrix for the turbulence state vector which turns out not to be positive definite. Since the succeeding state space and ARMA modelling of the turbulence rely on the positive definiteness of the cross-spectral density matrix, the problem with the non-positive definiteness of such matrices is at first addressed and suitable treatments regarding it are proposed. From the adjusted positive definite cross-spectral density matrix a frequency response matrix is constructed which determines the turbulence vector as a linear filtration of Gaussian white noise. Finally, an accurate state space modelling method is proposed which allows selection of an appropriate model order, and estimation of a state space model for the vector turbulence process incorporating its phase spectrum in one stage, and its results are compared with a conventional ARMA modelling method.

Keywords—Turbulence, wind turbine, complex coherence, state space modelling, ARMA modelling.

I. Introduction

TURBULENCE modelling has been of considerable interest for civil engineers during past decades. For large and flexible structures such as tall buildings, long span bridges and more specifically for wind turbines. Various modelling methods for simulation of a turbulent wind field are already suggested i.e. Fourier Analysis, Principal Components Analysis, ARMA modelling etc. [1]–[3]. Among the proposed methods, ARMA models have received considerable attention specifically due to their short memory requirement. An ARMA model is especially advantageous since the simulated turbulence vector is not periodic with time which is the case for spectral methods such as Fourier Analysis. ARMA models are reported to be quite successful in modelling wind field as long as the coherence function between discretized nodal points on the plane is assumed to be real, [3]. However their capability for modelling stochastic wind field with complex coherence function, which is the aim of this investigation, has not yet been demonstrated. Any stochastic process in the so-called parametric modelling class, in which a closed form function is estimated for generating the process, can be represented as either an ARMA model or a state space model. Indeed the state space formulation is merely an alternative, and sometimes more efficient, way of representing an ARMA model and both are convertible to each other. State space modelling of wind is already considered in this field, [4], and is reported to be numerically efficient and robust. Nevertheless as stated by Kareem, [3], there has been difficulties for the researchers in the field to find a proper general method for state space modelling of the phenomenon. In this paper a state space modelling method is introduced which overcomes these difficulties.

M.T.Sichani is with the Department of Civil Engineering, Aalborg University, 9000 Aalborg, DK e-mail: mts@civil.aau.dk
B.J.Pedersen is with LAC Engineering A/S, Bogøvej 15, DK-8382 Hinnerup e-mail: bjp@lacengineering.dk
S.R.K. Nielsen is with the Department of Civil Engineering, Aalborg University, 9000 Aalborg, DK e-mail: srkn@civil.aau.dk

The basic assumption is that the cross-spectral density function of the along wind turbulence component is available over the surface of the structure. Further the turbulence field is assumed to be spatial homogeneous and stationary in time. Next, the turbulence field is discretized in a number of nodal points as shown in Figure 2. The approach is illustrated with an empirical cross-spectral density function, where the auto-spectral density function is given by Kaimal power spectrum [5] and the complex coherence function is taken from Shiotani and Iwayani [6]. An important issue is the lack of positive definiteness of the cross spectral density matrix of the turbulence vector at low angular frequencies. Positive definiteness is essential in order to achieve numerical stability of the suggested ARMA and the state space models. Therefore, two modification schemes are proposed which guarantee positive definiteness of the modified cross spectral density matrix. The modified cross-spectral density matrix is then used to estimate an impulse response matrix which provides the turbulence vector by a convolution with a Gaussian white noise with independent unit intensity component processes. The indicated impulse response matrix is not causal, which is of great conceptual importance, since it shows that the ARMA model and the state space models, which make implicit use of causality of the process, approximate the original acausal process with a causal equivalent. Finally, a stochastic subspace State Space Modelling (SSM) method is applied. The method takes advantage of singular value decomposition as a numerical tool to estimate the optimum model order of the state space model in one stage. A numerical simulations is carried out to study the accuracy of the SSM method. In the example an ARMA model is calibrated based on the 2SLS method by Samaras et al., [7] and compared with the state space model of the SSM. It is concluded that the suggested state space modelling method provides substantial improvements.

II. Turbulence model

The mean wind and the turbulence field are described in the $(z_1, z_2, z_3)-$ coordinate system with origin in the lower left corner of the building. The z_1-axis is horizontal, along-wind direction. The, z_3-axis is the height from the ground, See Figure 1. The mean wind velocity V is assumed to be co-directional to the z_1-axis, and is considered constant over

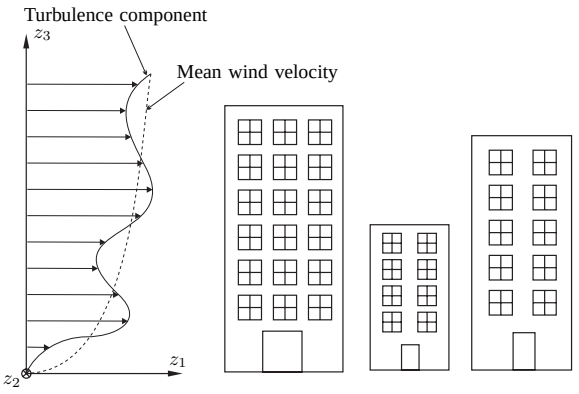

Fig. 1: Along wind variation of wind field with height.

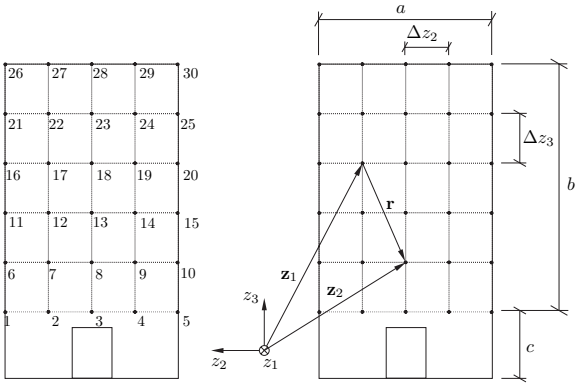

Fig. 2: Definition of nodes in numerical example.

the wind field area $A = ab$, where a is the dimension along z_2-axis and b is the dimension along z_3-axis. In what follows we shall only consider the turbulence component $v(\mathbf{z}, t)$ in the z_1-direction in neutral atmospheric turbulence at positions $\mathbf{z} = [z_1, z_2, z_3]$ in the discretized plane and at arbitrary times t. The turbulence field in the plane will be modelled as a zero-mean, Gaussian time-stationary process $\{v(\mathbf{z}, t),\ (\mathbf{z}, t) \in R^3 \times R\}$. Then, the turbulence process is completely determined by its cross-covariance function defined as, [8]

$$\kappa_{vv}(\mathbf{z}_1, t_1; \mathbf{z}_2, t_2) = E\big[v(\mathbf{z}_1, t_1)v(\mathbf{z}_2, t_2)\big] = \kappa_{vv}(\mathbf{r}, \tau) \quad (1)$$

$$\mathbf{r} = \mathbf{z}_2 - \mathbf{z}_1 \quad , \quad \tau = t_2 - t_1 \quad (2)$$

Where $E[\cdot]$ is the expectation operator, and $\mathbf{z}_1$ and $\mathbf{z}_2$ are the position vectors to two point in the discretized plane, see Figure 1. Alternatively, the correlation structure can be defined by the double-sided cross-spectral density function via the Wiener-Khintchine relation, [8]

$$S_{vv}(\mathbf{z}_1, \mathbf{z}_2; \omega) = \frac{1}{2\pi} \int_{-\infty}^{\infty} \mathrm{e}^{-i\omega t}\, \kappa_{vv}(\mathbf{z}_1, \mathbf{z}_2; \tau)\, d\tau \quad (3)$$

$S_{vv}(\mathbf{z}_1, \mathbf{z}_2; \omega)$ may be written on the form

$$S_{vv}(\mathbf{z}_1, \mathbf{z}_2; \omega) = \gamma_{vv}(\mathbf{z}_1, \mathbf{z}_2; \omega) S_{vv}^{\frac{1}{2}}(\mathbf{z}_1; \omega) S_{vv}^{\frac{1}{2}}(\mathbf{z}_2; \omega) \quad (4)$$

Where $\gamma_{vv}(\mathbf{z}_1, \mathbf{z}_2; \omega)$ is the so-called coherence function and $S_{vv}(\mathbf{z}; \omega)$ is the double-sided auto-spectral density of the turbulence. Due to the assumed homogeneity of the field over the wind field area the former depends on $\mathbf{z}_1$ and $\mathbf{z}_2$ via the difference $\mathbf{r} = \mathbf{z}_2 - \mathbf{z}_1$, and the latter is independent of the position vector $\mathbf{z}$. In the inertial sub-range of equilibrium range the double-sided auto-spectral density function may be given by the following empirical expression, [5]

$$\left.\begin{aligned} S_{vv}(\mathbf{r}; \omega) &= \frac{1}{V} F\left(\frac{\omega}{V}\right) \\ F(k) \quad &= \frac{\sigma_v^2}{\gamma} \frac{L}{\left(1 + |Lk|\right)^{5/3}} \end{aligned}\right\} \quad (5)$$

V is the mean wind velocity in the middle height of the building, which is assumed to be constant over the building face area. σ_v is the standard deviation of the turbulence, L is the correlation length, and γ is a normalization parameter given as

$$\left.\begin{aligned} \sigma_v &= 2.18\ V_* \\ L \ &= 5.25\, h \\ \gamma \ &= 3 \end{aligned}\right\} \quad (6)$$

V_* is the friction velocity given as $V_* = V_{10} k_t \kappa$, where V_{10} is the mean wind velocity at 10m, $k_t = 0.17$ is a friction coefficient, and $\kappa = 0.40$ is von Karman's constant. The cross-spectral density function fulfills the symmetry properties, [8]

$$S_{vv}(\mathbf{z}_1, \mathbf{z}_2; \omega) = S_{vv}^*(\mathbf{z}_2, \mathbf{z}_1; \omega) = S_{vv}^*(\mathbf{z}_1, \mathbf{z}_2; -\omega) \quad (7)$$

where $*$ denotes complex conjugation. Due to the homogeneity the coherence function merely depends on $\mathbf{z}_1$ and $\mathbf{z}_2$ via the difference vector $\mathbf{r} = \mathbf{z}_2 - \mathbf{z}_1$. Then due to (7), the coherence must fulfil the following asymptotic values and symmetry properties

$$\left.\begin{aligned} \gamma(\mathbf{r}; \omega) &= 1 \quad , \quad \mathbf{r} = \mathbf{0} \\ \gamma(\mathbf{r}; \omega) &= 0 \quad , \quad |\mathbf{r}| = \infty \\ \gamma(\mathbf{r}; \omega) &= \gamma^*(-\mathbf{r}; \omega) \\ \gamma(\mathbf{r}; \omega) &= \gamma^*(\mathbf{r}; -\omega) \end{aligned}\right\} \quad (8)$$

An empirical expression, which complies with the indicated requirements have been given by [6]

$$\gamma(\mathbf{r}; \omega) = \exp\left(-\frac{|\mathbf{r}||\omega|}{V} d_1\right) \exp\left(i \frac{\mathrm{s}(\mathbf{r})|\mathbf{r}|\,\omega}{V} d_2\right) \quad (9)$$

Where the sign function is defined so $\mathrm{s}(\mathbf{r}) = 1$ and $\mathrm{s}(-\mathbf{r}) = -1$. The non-dimensional parameters d_1 and d_2 are given as $d_1 \simeq 1.5$ and $d_2 \simeq 1.3$, [6].

III. Discretization of the turbulence field

The wind field area is divided by n segments of magnitude $\Delta z_2 = \frac{a}{n}$, see Figure 2. Along each side of a segment the radius R of the wind field area is divided into m equidistant intervals of the length $\Delta z_3 = \frac{b}{m}$, defining m nodes. The total number of nodes becomes $M = nm$, where the first node refers to the origin of the coordinate system. Then, the discretized field, representing the turbulence in the defined nodes may be represented by the stochastic vector

$$\mathbf{v}(t) = \begin{bmatrix} v(\mathbf{z}_1, t) \\ v(\mathbf{z}_2, t) \\ \vdots \\ v(\mathbf{z}_M, t) \end{bmatrix} = \begin{bmatrix} v_1(t) \\ v_2(t) \\ \vdots \\ v_M(t) \end{bmatrix} \tag{10}$$

The double-sided cross-spectral density matrix of the turbulence vector becomes

$$\mathbf{S_{vv}}(\omega) = \begin{bmatrix} S_{vv}(\mathbf{z}_1, \mathbf{z}_1; \omega) & \cdots & S_{vv}(\mathbf{z}_1, \mathbf{z}_M; \omega) \\ S_{vv}(\mathbf{z}_2, \mathbf{z}_1; \omega) & \cdots & S_{vv}(\mathbf{z}_2, \mathbf{z}_M; \omega) \\ \vdots & \ddots & \vdots \\ S_{vv}(\mathbf{z}_M, \mathbf{z}_1; \omega) & \cdots & S_{vv}(\mathbf{z}_M, \mathbf{z}_M; \omega) \end{bmatrix} \tag{11}$$

$\mathbf{S_{vv}}(\omega)$ is a Hermitian matrix fulfilling the symmetry properties

$$\mathbf{S_{vv}}(\omega) = \mathbf{S}_{\mathbf{vv}}^{\mathrm{T}*}(\omega) = \mathbf{S}_{\mathbf{vv}}^{*}(-\omega) \tag{12}$$

Using the symmetry property (12) the cross-covariance matrix of the turbulence vector may be obtained from the following Finite Fourier Transform

$$\begin{aligned} \mathbf{C_{vv}}(\tau) = \textstyle\int_{-\infty}^{\infty} \mathrm{e}^{i\omega\tau}\, \mathbf{S_{vv}}(\omega)\, d\omega = \\ 2\mathrm{Re}\left(\textstyle\int_{0}^{\infty} \mathrm{e}^{i\omega\tau}\, \mathbf{S_{vv}}(\omega)\, d\omega\right) \quad \Rightarrow \\ \mathbf{C_{vv}}(j) \simeq 2\Delta\omega \mathrm{Re}\left(\textstyle\sum_{k=0}^{N-1} \exp\left(i2\pi\frac{jk}{N}\right)\, \mathbf{S_{vv}}(k)\right) \end{aligned} \tag{13}$$

where $j = 0, 1, \ldots, N-1$. The abbreviated notations $\mathbf{C_{vv}}(j) = \mathbf{C_{vv}}(j\Delta\tau)$ and $\mathbf{S_{vv}}(k) = \mathbf{S_{vv}}(k\Delta\omega)$ have been introduced, and where the time and frequency increments are related as $\Delta\tau\Delta\omega = \frac{2\pi}{N}$. $\mathbf{S_{vv}}(\omega)$ may be Gauss factorized on the form

$$\mathbf{S_{vv}}(\omega) = \mathbf{L}^{*}(\omega)\, \mathbf{D}(\omega)\, \mathbf{L}^{\mathrm{T}}(\omega) \tag{14}$$

where $\mathbf{L}(\omega)$ is a lower triangular complex matrix with 1 in the main diagonal, and $\mathbf{D}(\omega)$ is a real diagonal matrix. Since, $\mathbf{S_{vv}}(\omega)$ is not necessarily positive definite the diagonal components need not be positive real. If not so, we may define an auxiliary diagonal matrix $\tilde{\mathbf{D}}(\omega)$, in which the negative components of $\mathbf{D}(\omega)$ is set to zero. Correspondingly, the following positive semi-definite cross spectral density matrix may be constructed

$$\tilde{\mathbf{S}}_{\mathbf{vv}}(\omega) = \mathbf{L}^{*}(\omega)\, \tilde{\mathbf{D}}(\omega)\, \mathbf{L}^{\mathrm{T}}(\omega) \tag{15}$$

$\tilde{\mathbf{S}}_{\mathbf{vv}}(\omega)$ may be factorized on the form

$$\tilde{\mathbf{S}}_{\mathbf{vv}}(\omega) = \mathbf{H}_{\mathbf{v}}^{*}(\omega)\mathbf{H}_{\mathbf{v}}^{\mathrm{T}}(\omega) \tag{16}$$

where

$$\mathbf{H_v}(\omega) = \mathbf{L}^{*}(\omega)\tilde{\mathbf{D}}^{\frac{1}{2}}(\omega) \tag{17}$$

$\tilde{\mathbf{D}}^{\frac{1}{2}}(\omega)$ is a diagonal matrix with the square root of $\mathbf{D}^{\frac{1}{2}}(\omega)$ on the main diagonal. $\mathbf{H_v}(\omega)$ has the form of a lower complex triangular matrix

$$\mathbf{H_v}(\omega) = \begin{bmatrix} H_{11}(\omega) & 0 & \cdots & 0 \\ H_{21}(\omega) & H_{22}(\omega) & \cdots & 0 \\ \vdots & \vdots & \ddots & \vdots \\ H_{M\,1}(\omega) & H_{M\,2}(\omega) & \ldots & H_{M\,M}(\omega) \end{bmatrix} \tag{18}$$

Obviously the columns of $\mathbf{H_v}(\omega)$ corresponding to the elements in the diagonal of $\tilde{\mathbf{D}}^{\frac{1}{2}}(\omega)$ set to zero become zero as well. Hence the factorization (16) corresponds the modified Cholesky algorithm suggested by Shinozuka and Jan [1].

Alternatively, the following eigenvalue decomposition may be considered

$$\mathbf{S_{vv}}(\omega) = \mathbf{\Psi}(\omega)\, \mathbf{\Lambda}(\omega)\, \mathbf{\Psi}^{*\mathrm{T}}(\omega) \tag{19}$$

where $\mathbf{\Psi}(\omega)$ is a modal matrix storing the eigenvectors of $\mathbf{S_{vv}}(\omega)$ column wise, and $\mathbf{\Lambda}$ is a diagonal matrix storing the corresponding eigenvalues. Notice, the formulation (19) assumes that the eigenvectors have been normalized to unit length in which case $\mathbf{\Psi}^{-1}(\omega) = \mathbf{\Psi}^{*\mathrm{T}}(\omega)$. Next, the negative and zero eigenvalues in $\mathbf{\Lambda}(\omega)$ are set to a small positive number, e.g. $\varepsilon = 10^{-10}$, providing a modified eigenvalue matrix $\tilde{\mathbf{\Lambda}}(\omega)$, from which the following positive definite cross-spectral density matrix may be constructed

$$\tilde{\mathbf{S}}_{\mathbf{vv}}(\omega) = \mathbf{\Psi}(\omega)\, \tilde{\mathbf{\Lambda}}(\omega)\, \mathbf{\Psi}^{*\mathrm{T}}(\omega) \tag{20}$$

Finally, the lower triangular matrix $\mathbf{H_v}(\omega)$ might be obtained by a Cholesky decomposition of (20). The matrices $\mathbf{H_v}(\omega)$ obtained by the two methods are not identical. The latter approach turns out to introduce smaller errors in the constructed positive definite cross-spectral density matrix compared to the target spectrum, as demonstrated in the numerical example. This improvement is obtained at the cost of a significant increase in the computational expenses. Notice, in both cases $\mathbf{S_{vv}}(\omega)$ and $\tilde{\mathbf{S}}_{\mathbf{vv}}(\omega)$ only differ at angular frequencies, where the former is not positive definite. The symmetry property $\mathbf{S_{vv}}(\omega) = \mathbf{S}_{\mathbf{vv}}^{*}(-\omega)$ implies that the following symmetry property prevails for $\mathbf{H_v}(\omega)$

$$\mathbf{H_v}(\omega) = \mathbf{H}_{\mathbf{v}}^{*}(-\omega) \tag{21}$$

Let $\{\mathbf{u}(t),\ t \in R\}$ denote an M-dimensional white vector noise process with the double-sided cross-spectral density and cross-covariance matrices given as

$$\mathbf{S_{uu}}(\omega) = \mathbf{I} \tag{22}$$

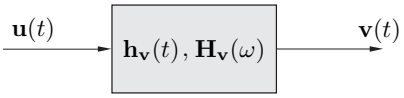

Fig. 3: Turbulence vector **v**(t) as a linear filtration of a Gaussian white noise vector $\mathbf{u}(t)$.

$$\mathbf{C_{uu}}(\tau) = 2\pi\delta(\tau)\,\mathbf{I} \tag{23}$$

The related impulse response matrix $\mathbf{h_v}(t)$ is the inverse Fourier transform of $\mathbf{H_v}(\omega)$. Using the symmetry property (21) $\mathbf{h_v}(t)$ may be determined by the following Finite Fourier Transform

$$\begin{aligned} \mathbf{h_v}(t) = \tfrac{1}{2\pi}\int_{-\infty}^{\infty} \mathrm{e}^{i\omega t}\,\mathbf{H_v}(\omega)\,d\omega = \\ \tfrac{1}{\pi}\,\mathrm{Re}\left(\int_0^{\infty} \mathrm{e}^{i\omega t}\,\mathbf{H_v}(\omega)\,d\omega\right) \quad \Rightarrow \\ \mathbf{h_v}(j) = \tfrac{\Delta\omega}{\pi}\mathrm{Re}\left(\sum_{k=0}^{N-1}\exp\left(i2\pi\tfrac{jk}{N}\right)\,\mathbf{H_v}(k)\right) \end{aligned} \tag{24}$$

where $j = 0, 1, \ldots, N-1$. $\mathbf{h_v}(t)$ becomes a lower triangular matrix similar to $\mathbf{H_v}(\omega)$. The causality condition is generally not fulfilled, i.e. $\mathbf{h_v}(t) \neq \mathbf{0},\ t < 0$. Notice that $\mathbf{h_v}(-j) = \mathbf{h_v}(N-j)$, and hence is available from (24) up to the Nyquist frequency $N/2$.

IV. ARMA MODELLING

In principle, simulation of the turbulence vector may be based on convolving its impulse response function by a proper Gaussian white noise, c.f. Figure 3. However, $\mathbf{h_v}(l)$ converges to zero very slowly with l as seen in Figure 6 below. This truncation error together with numerical integration error introduced by (24) in estimation of $\mathbf{h_v}(l)$, cause discrepancy of the variance function of $\mathbf{h_v}(l)$ with (13). Hence N should be very large to keep Δt at an acceptable level. To circumvent this problem an equivalent ARMA vector model with finite lengths p and q of the auto-regressive and moving average parts might be applied corresponding to the model

$$\mathbf{v}(k) + \sum_{l=1}^{p}\mathbf{A}_l\mathbf{v}(k-l) = \sum_{l=0}^{q}\mathbf{B}_l\mathbf{w}(k-l) \tag{25}$$

where $\mathbf{A}_l$ and $\mathbf{B}_l$ are real matrices of dimension $M \times M$. Following the suggestion of Samaras et al. [7] the Two Stage Least Square (2SLS) method of Gersch and Liu [9] will at first be used to estimate $\mathbf{A}_l$ and $\mathbf{B}_l$ of (25). The algorithm consists of two major steps; in the first step an AR model of sufficiently high order $\acute{p}$ is calibrated for the process, and in the second step the obtained AR model is approximated by a shorter ARMA(p,q) model. To guarantee sufficient accuracy of the modelling, Samaras et.al. [7] proposed to choose $\acute{p} \geq p+q+2$, whereas Li and Kareem [10] proposed the empirical relation $\acute{p} \geq 3(p+q)$

$$\mathbf{v}(k) + \sum_{l=1}^{\acute{p}}\tilde{\mathbf{A}}_l\mathbf{v}(k-l) = \mathbf{B}_0\mathbf{w}(k) \tag{26}$$

To calibrate $\tilde{\mathbf{A}}_l$ coefficients, (26) is post multiplied by $\mathbf{v}^{\mathrm{T}}(k-j), k = 1, 2, \cdots$ and its expectation is taken which yields in (27)

$$\mathbf{C}^{\mathrm{T}}_{\mathbf{vv}}(j) + \sum_{l=1}^{\acute{p}}\tilde{\mathbf{A}}_l\mathbf{C}^{\mathrm{T}}_{\mathbf{vv}}(j-l) = \mathbf{0} \quad , \quad j = 1, 2, \cdots \tag{27}$$

where $\mathbf{C_{vv}}(j) = \mathbf{C}^{\mathrm{T}}_{\mathbf{vv}}(-j)$ is used. Along with $E[\mathbf{w}(j)\mathbf{v}^{\mathrm{T}}(j-k)] = \mathbf{0}$ for $k > 0$ according to the causality of the model. Evaluating (27) for $j = 1, \cdots, \acute{p}$ allows calibration of $\tilde{\mathbf{A}}_l$ in a least square sense. Next post multiplying (26) by $\mathbf{w}^{\mathrm{T}}(k)$ and taking its expectation results in

$$\mathbf{C_{vw}}(0) = 2\pi\Delta t\mathbf{B}_0 \tag{28}$$

Post multiplying (26) by $\mathbf{v}^{\mathrm{T}}(k)$ and taking its expectation together with using (28) provides the following identity, which will be used to estimate $\mathbf{B}_0\mathbf{B}_0^{\mathrm{T}}$

$$\mathbf{C}^{\mathrm{T}}_{\mathbf{vv}}(0) + \sum_{l=1}^{\acute{p}}\tilde{\mathbf{A}}_l\mathbf{C}^{\mathrm{T}}_{\mathbf{vv}}(-l) = 2\pi\Delta t\mathbf{B}_0\mathbf{B}_0^{\mathrm{T}} \tag{29}$$

(29) is used for the estimation of $\mathbf{B}_0$ by performing a Cholesky decomposition of $\mathbf{B}_0\mathbf{B}_0^{\mathrm{T}}$. The next step of the method is to calibrate an ARMA(p,q) model that fits at best to the estimated high order AR model. Therefore the second least square approximation is merely used for shortening the memory of the model. Consequently the high order AR model is the more accurate of the two. This is the reason why the performance of the high order AR model of the 2SLS method is compared with that of the estimated state space method formulated below. In the simulation, the covariance function of the 2SLS method is calculated recursively using equation (27).

V. STOCHASTIC SUBSPACE MODELLING

In this section an stochastic subspace outline of the State Space Modelling (SSM) method and the stochastic realization theory is given. In general, a stochastic process in state space is represented by (30)

$$\begin{aligned} \mathbf{x}(j+1) &= \mathbf{A}\mathbf{x}(j) + \mathbf{\Theta}(j) \\ \mathbf{v}(j) &= \mathbf{C}\mathbf{x}(j) + \mathbf{\Phi}(j) \end{aligned} \tag{30}$$

where the auxiliary state vector $\mathbf{x}(j)$ is of dimension $L \times 1$, and $\mathbf{\Theta}(j)$ and $\mathbf{\Phi}(j)$ are stationary Gaussian white noise vector processes of the dimension $L \times 1$ and $M \times 1$, respectively. $\mathbf{A}$ is a system matrix of the dimension $L \times L$ and $\mathbf{C}$ is an observation matrix of the dimension $M \times L$. The cross-covariance matrices of the stochastic sequences $\{\mathbf{\Theta}(j)\}$ and $\{\mathbf{\Phi}(j)\}$ are given as

$$E\left[\begin{bmatrix}\mathbf{\Theta}(j)\\ \mathbf{\Phi}(j)\end{bmatrix}\begin{bmatrix}\mathbf{\Theta}^{\mathrm{T}}(k) & \mathbf{\Phi}^{\mathrm{T}}(k)\end{bmatrix}\right] = \begin{bmatrix}\mathbf{Q} & \mathbf{S}\\ \mathbf{S}^{\mathrm{T}} & \mathbf{R}\end{bmatrix}\delta_{jk} \tag{31}$$

where δ_{jk} is the Kronecker delta. The idea of the state space modelling is to estimate the zero time-lag noise covariance matrices $\mathbf{Q}$ of dimension $L \times L$, $\mathbf{R}$ of dimension $M \times M$

and $\mathbf{S}$ of dimension $M \times L$ along with system matrices $\mathbf{A}$ of dimension $L \times L$ and $\mathbf{C}$ of dimension $M \times L$, so the output process $\mathbf{v}(j)$ satisfies a given target cross-covariance matrix $\mathbf{C_{vv}}(j)$. Katayama [13] has shown that the state space model (30) might be transformed to the following so-called forward innovation model admitting the standard form of a Kalman filter

$$\begin{aligned} \bar{\mathbf{x}}(j+1) &= \mathbf{A}\bar{\mathbf{x}}(j) + \mathbf{K}(j)\mathbf{e}(j) \\ \mathbf{v}(j) &= \mathbf{C}\bar{\mathbf{x}}(j) + \mathbf{e}(j) \end{aligned} \tag{32}$$

where $\mathbf{K}(j)$ is a set of non-steady state Kalman filter gain matrices, and $\{\mathbf{e}(j)\}$ is a zero-mean non-stationary white noise vector sequence. The forward innovation model (32) has two outstanding privileges over (30). First, it has less redundancy in the noise terms, since they are related to each other through the Kalman gain matrix $\mathbf{K}(j)$. Second, accuracy of the modelling requires that the states of the model are estimated with the least possible error compared to the true states of the system, [11], which is known to be possible via using a Kalman filter. Notice that whereas the state vector and the noise processes are affected by the transformation, the output vector $\{\mathbf{v}(j)\}$ is not changed. Further, it is assumed that the state vector of (32) has deterministic start $\bar{\mathbf{x}}(0) = \mathbf{0}$. As a consequence, both $\{\bar{\mathbf{x}}(j)\}$ and $\{\mathbf{v}(j)\}$ become zero-mean non-stationary Gaussian processes. Then, the initial value of the cross-covariance matrix of the state vector, $\bar{\mathbf{\Sigma}}(j) = E[\bar{\mathbf{x}}(j)\bar{\mathbf{x}}^{\mathrm{T}}(j)]$, becomes $\bar{\mathbf{\Sigma}}(0) = \mathbf{0}$. The Kalman gain matrix in (32) is time dependent in general, while as $j \to \infty$, it approaches a stationary value $\mathbf{K} = \mathbf{K}(\infty)$. Next, the state covariance matrix will also approach a stationary value $\bar{\mathbf{\Sigma}} = \bar{\mathbf{\Sigma}}(\infty)$. The following equations for the mean value and covariance of the states of (32) are then derived

$$E[\bar{\mathbf{x}}(j)] = \mathbf{0} \tag{33}$$

$$E[\bar{\mathbf{x}}(j)\bar{\mathbf{x}}^{\mathrm{T}}(j)] = \bar{\mathbf{\Sigma}} \tag{34}$$

$$E[\bar{\mathbf{x}}(j)\mathbf{e}^{\mathrm{T}}(j)] = \mathbf{0} \tag{35}$$

The second equation of (32) estimates the noise cross-covariance matrix, $\mathbf{R}_K = E[\mathbf{e}(j)\mathbf{e}^{\mathrm{T}}(j)]$, as

$$\mathbf{R}_K = \mathbf{C}_{\mathbf{vv}}^{\mathrm{T}}(0) - \mathbf{C}\bar{\mathbf{\Sigma}}\mathbf{C}^{\mathrm{T}} \tag{36}$$

Now the statement of the problem is to find the quadruple $\{\mathbf{A}, \mathbf{C}, \mathbf{K}, \mathbf{R}_K\}$ such that the specified covariance matrices are satisfied by the output process. The covariance matrix between the next state vector and the present output vector, $\bar{\mathbf{G}}^{\mathrm{T}}(j) = E[\bar{\mathbf{x}}(j+1)\mathbf{v}^{\mathrm{T}}(j)]$, and the output covariance matrix $\mathbf{C}_{\mathbf{vv}}^{\mathrm{T}}(i) = E[\mathbf{v}(j+i)\mathbf{v}^{\mathrm{T}}(j)]$ for model (32) are given as

$$\begin{aligned} \bar{\mathbf{G}}^{\mathrm{T}} &= \mathbf{A}\bar{\mathbf{\Sigma}}\mathbf{C}^{\mathrm{T}} + \mathbf{K}\mathbf{R}_K \\ \mathbf{C}_{\mathbf{vv}}^{\mathrm{T}}(0) &= \mathbf{C}\bar{\mathbf{\Sigma}}\mathbf{C}^{\mathrm{T}} + \mathbf{R}_K \\ \mathbf{C}_{\mathbf{vv}}^{\mathrm{T}}(i) &= \mathbf{C}\mathbf{A}^{i-1}\bar{\mathbf{G}}^{\mathrm{T}} \end{aligned} \tag{37}$$

From (37), (32) and (36) the following general discrete algebraic Riccati equation can be derived and solved for the development of $\bar{\mathbf{\Sigma}}$

$$\begin{aligned} \bar{\mathbf{\Sigma}} &= \mathbf{A}\bar{\mathbf{\Sigma}}\mathbf{A}^{\mathrm{T}} + (\bar{\mathbf{G}}^{\mathrm{T}} - \mathbf{A}\bar{\mathbf{\Sigma}}\mathbf{C}^{\mathrm{T}}) \\ &\quad \times (\mathbf{C}_{\mathbf{vv}}^{\mathrm{T}}(0) - \mathbf{C}\bar{\mathbf{\Sigma}}\mathbf{C}^{\mathrm{T}})^{-1}(\bar{\mathbf{G}}^{\mathrm{T}} - \mathbf{A}\bar{\mathbf{\Sigma}}\mathbf{C}^{\mathrm{T}})^{\mathrm{T}} \end{aligned} \tag{38}$$

Therefore if $\{\mathbf{A}, \mathbf{C}, \bar{\mathbf{G}}^{\mathrm{T}}\}$ are available, it is required to solve (38) only once to obtain $\bar{\mathbf{\Sigma}}$. There exist various methods for solving the indicated Riccati equation; among them the algorithm by [11] is employed in the current work. Next, $\mathbf{R}_K$ is calculated using (36). The stationary Kalman gain matrix $\mathbf{K}$ is estimated from

$$\mathbf{K} = (\bar{\mathbf{G}}^{\mathrm{T}} - \mathbf{A}\bar{\mathbf{\Sigma}}\mathbf{C}^{\mathrm{T}})\mathbf{R}_K^{-1} \tag{39}$$

Knowledge of the quadruple $\{\mathbf{A}, \mathbf{C}, \mathbf{K}, \mathbf{R}_K\}$ is sufficient for constructing a state space model in the form of (32) capable of generating a stochastic process with any specified covariance function.

A. System realization theory

The so-called realization algorithm is used as the starting point to estimate the triplet $\{\mathbf{A}, \mathbf{C}, \bar{\mathbf{G}}^{\mathrm{T}}\}$ which are then used to estimate $\bar{\mathbf{\Sigma}}$ and $\mathbf{K}$. At first the block Toeplitz matrix $\mathbf{T}$ of the cross-covariance matrices of the outputs, of dimension $Mi \times Mi$ is constructed

$$\mathbf{T} = \begin{bmatrix} \mathbf{C}_{\mathbf{vv}}^{\mathrm{T}}(i) & \mathbf{C}_{\mathbf{vv}}^{\mathrm{T}}(i-1) & \cdots & \mathbf{C}_{\mathbf{vv}}^{\mathrm{T}}(1) \\ \mathbf{C}_{\mathbf{vv}}^{\mathrm{T}}(i+1) & \mathbf{C}_{\mathbf{vv}}^{\mathrm{T}}(i) & \cdots & \mathbf{C}_{\mathbf{vv}}^{\mathrm{T}}(2) \\ \vdots & \vdots & \ddots & \vdots \\ \mathbf{C}_{\mathbf{vv}}^{\mathrm{T}}(2i-1) & \mathbf{C}_{\mathbf{vv}}^{\mathrm{T}}(2i-2) & \cdots & \mathbf{C}_{\mathbf{vv}}^{\mathrm{T}}(i) \end{bmatrix} \tag{40}$$

Referring to (37) it is clear that $\mathbf{T}$ can be constructed as the product of an extended observability matrix $\mathbf{O}$ of dimension $Mi \times L$ and the reversed extended stochastic controllability matrix $\mathbf{P}$ of dimension $L \times Mi$ defined below

$$\mathbf{T} = \mathbf{O}\,\mathbf{P} = \begin{bmatrix} \mathbf{C} \\ \mathbf{C}\mathbf{A} \\ \vdots \\ \mathbf{C}\mathbf{A}^{i-1} \end{bmatrix} \begin{bmatrix} \mathbf{A}^{i-1}\bar{\mathbf{G}}^{\mathrm{T}} & \cdots & \mathbf{A}\bar{\mathbf{G}}^{\mathrm{T}} & \bar{\mathbf{G}}^{\mathrm{T}} \end{bmatrix} \tag{41}$$

The phrase extended observability matrix is used, since in general the number of block rows of the matrix is longer than the number of system states, i.e. $i > L$. The same explanation holds for the reversed extended stochastic controllability matrix. The strategy to estimate $\mathbf{O}$ and $\mathbf{P}$ in the next step is to decompose $\mathbf{T}$ into its singular values, sorted in a monotone non-increasing manner, and their corresponding singular vectors in the following way

$$\mathbf{T} = \begin{bmatrix} \mathbf{U}_1 & \mathbf{U}_2 \end{bmatrix} \begin{bmatrix} \mathbf{S}_1 & \mathbf{0} \\ \mathbf{0} & \mathbf{S}_2 \end{bmatrix} \begin{bmatrix} \mathbf{V}_1^{\mathrm{T}} \\ \mathbf{V}_2^{\mathrm{T}} \end{bmatrix} \tag{42}$$

$\mathbf{S}_1$ of dimension $r \times r$ is a diagonal matrix consisting of the first *r* singular values, $\mathbf{U}_1$ of dimension $Mi \times r$ is the block of the left singular vectors corresponding to $\mathbf{S}_1$ and

$\mathbf{V}_1^{\mathrm{T}}$, of dimension $r \times Mi$, is its corresponding block of right singular vectors. On the condition that system is stable - all of the eigenvalues of the matrix $\mathbf{A}$ are inside unit circle - and the system is excited by white noise, $\mathbf{T}$ will have just *r* non-zero singular values which equals the system order, [11]. In such circumstances $r = L$, and $\mathbf{S}_2 = \mathbf{0}$ is a square matrix of dimension $(Mi - r) \times (Mi - r)$. The extended observability and the reversed extended stochastic controllability can then be estimated as follows

$$\hat{\mathbf{O}} = \mathbf{U}_1 \mathbf{S}_1^{1/2} \quad , \quad \hat{\mathbf{P}} = \hat{\mathbf{O}}^{\dagger} \mathbf{T} \tag{43}$$

Here $()^{\dagger}$ denotes the pseudo inverse of the matrix. Although it is possible to use different fractions of the singular values for estimation of $\mathbf{O}$ and $\mathbf{P}$, the benefit of the proposed decomposition is that it causes controllability and observability of the estimated system to be balanced, [11], [13]. Balancing here means that the number of controllable and observable states of the system are equal. In what follows the hat sign over matrixes shows that they are estimations of the original matrix. Next $\hat{\mathbf{C}}$ might be chosen as the first *M* rows of $\hat{\mathbf{O}}$ and $\hat{\bar{\mathbf{G}}}^{\mathrm{T}}$ as the last *M* columns of $\hat{\mathbf{P}}$. Next, defining $\hat{\mathbf{O}}^{\downarrow}$ of dimension $(M-1)i \times L$ by stripping last *M* rows of $\hat{\mathbf{O}}$, and $\hat{\mathbf{O}}^{\uparrow}$ of dimension $(M-1)i \times L$ by stripping first *M* rows of $\hat{\mathbf{O}}$, equation (44) might be used to calculate $\hat{\mathbf{A}}$ in an over-determined set of equations as

$$\hat{\mathbf{A}} = \left[\hat{\mathbf{O}}^{\downarrow}\right]^{\dagger} \hat{\mathbf{O}}^{\uparrow} \tag{44}$$

$\{\hat{\mathbf{A}}, \hat{\mathbf{C}}, \hat{\bar{\mathbf{G}}}^{\mathrm{T}}\}$ can then be used together with (38) and (39) to calculate $\hat{\bar{\mathbf{\Sigma}}}$ and $\hat{\mathbf{K}}$ respectively. Equation (37) might be used to calculate the cross covariance matrices of the estimated state space model. A very good approximation of a proper model order can be made by investigating the magnitude of the singular values of $\mathbf{T}$. According to the theory, there should be r non-zero singular values which specify the model order, and the rest of the singular values should be zero. In practice, for instance in vector turbulence modelling, it is most often the case that singular values gradually decrease to zero, see Figure 8. Therefore the optimum model order, i, is usually chosen so either $s_i \gg s_{i+1}$ or $s_{i+1} \approx 0$, where s_i is the i^{th} singular value.

B. Remarks on the algorithm

There exist three important conditions that any state space model must satisfy. First, the model must be stable, therefore all of the eigenvalues of $\hat{\mathbf{A}}$ must be located inside the unit circle in the complex plane. Second, the state covariance matrix $\bar{\mathbf{\Sigma}}$ must be symmetric and positive semi-definite. Third, the estimated noise covariance matrix by (36) must be symmetric and positive definite. The stability of the model is the most sensitive of the three and occasionally seen not satisfied in practice, which is also pointed out by Li and Kareem [10]. Therefore it is necessary to check them to guarantee feasibility of the model.

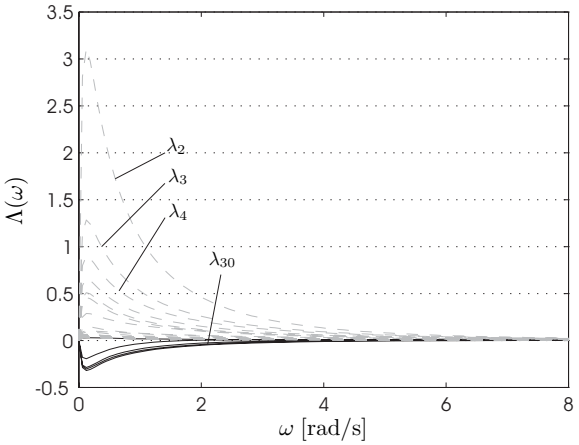

Fig. 4: Eigenvalues of the cross-spectral density matrix.

$$\mathbf{C}_{\mathbf{w}_s \mathbf{w}_s}(k-j) = E\left[\mathbf{w}_s(j)\mathbf{w}_s^{\mathrm{T}}(k)\right] = \begin{cases} \mathbf{0} & , \quad j \neq k \\ \mathbf{I} & , \quad j = k \end{cases} \tag{45}$$

Furthermore, define a lower triangular matrix $\mathbf{\Gamma}$, obtained by Cholesky decomposition of the noise covariance matrix given by (36). Then the white noise vector sequence in (32) might be generated as $\mathbf{e}(j) = \mathbf{\Gamma}\mathbf{w}_s(j)$. In which $\mathbf{w}_s(j)$ is a zero mean stationary Gaussian white noise vector of dimension $M \times 1$ with mutually independent random variables and cross covariance matrix indicated by (45).

VI. Numerical simulation

The along-wind turbulence will be simulated in the 30 nodes indicated in Figure 2. Dimensions of the turbulence field are chosen $a = c = 30m, b = 60m, \Delta z_2 = 7.5m$ and $\Delta z_3 = 12m$. The mean wind velocity is assumed to be constant over the wind field area and is given as $V = 15\,[\mathrm{m/s}]$. Simulation parameters are chosen as $N = 2048$ and $\Delta t = 0.0488s$. Figure 4 shows the eigenvalues of the cross-spectral density matrix of the turbulence as a function of the frequency. The first eigenvalue, within the demonstrated frequency range, is about three orders of magnitude larger than the second one if sorted in a decrementing order. Therefore the first eigenvalue is not plotted to allow detail investigation of the behavior of the other eigenvalues. Figure 5 illustrates the accuracy of the modified cross-spectral density matrix $\tilde{\mathbf{S}}_{\mathbf{vv}}(\omega)$ defined by (15) and (20), respectively, in comparison to the corresponding unmodified matrix $\mathbf{S}_{\mathbf{vv}}(\omega)$. The figure shows the relative error of $\tilde{\mathbf{S}}_{\mathbf{vv}}(\omega)$ compared to $\mathbf{S}_{\mathbf{vv}}(\omega)$ as expressed by the fractions of Eucledian norms $\| \tilde{\mathbf{S}}_{\mathbf{vv}}(\omega) - \mathbf{S}_{\mathbf{vv}}(\omega) \| / \| \mathbf{S}_{\mathbf{vv}}(\omega) \|$ as a function of the angular frequency in the interval $\omega \in [0, 6.5s^{-1}]$, where non-positive definiteness of $\tilde{\mathbf{S}}_{\mathbf{vv}}(\omega)$ occurs. As seen the normalized error related to the modification (15) may be up to 100% at some frequencies. In contrast the modification (20) is related to much smaller errors.

Figure 6 shows the components $h_{11}(t)$ related to node 1 on figure 2, and the cross function $h_{21}(t)$ between nodes 2 and 1

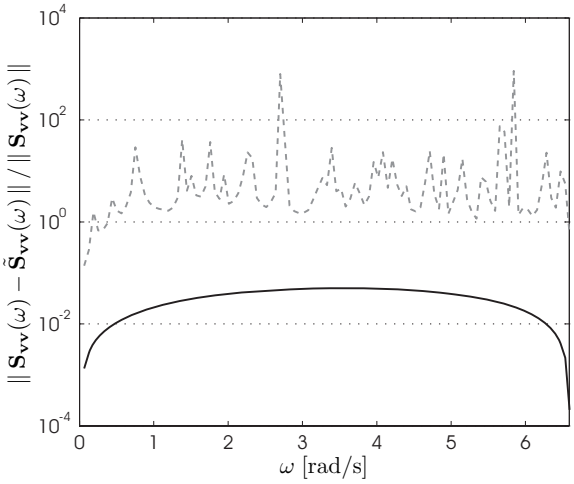

Fig. 5: Relative error of Eucledian norm of modified cross-spectral density matrix. —:$\tilde{\mathbf{S}}_{\mathbf{vv}}(\omega)$ given by Eq. (20). – – –:$\tilde{\mathbf{S}}_{\mathbf{vv}}(\omega)$ given by Eq. (15).

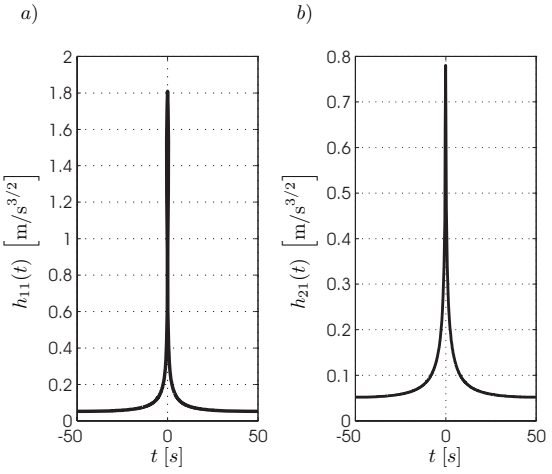

Fig. 6: Components of the impulse response matrix. a) $h_{11}(t)$. b) $h_{21}(t)$.

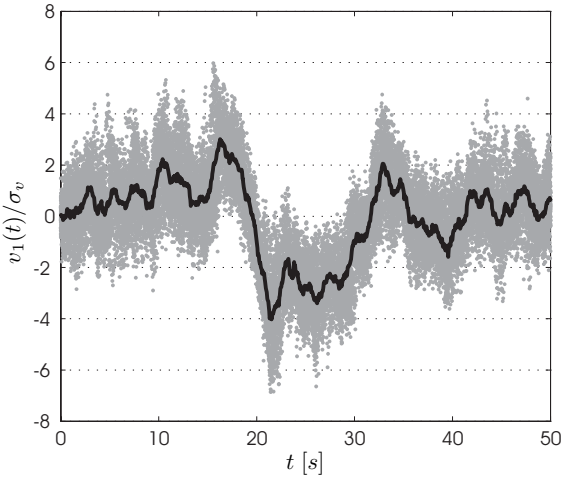

Fig. 7: Numerical simulation of turbulence field based on AR model, Eq. (26). —: Spatial mean of the turbulence realizations. ·: Spatial distribution of the turbulence realizations.

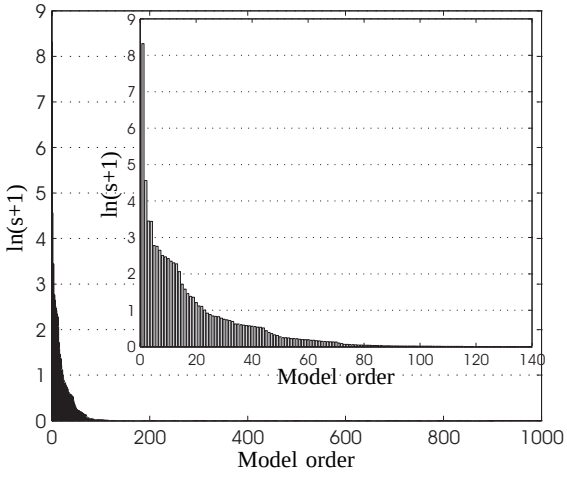

Fig. 8: Singular values of the block Toeplits matrix of the cross-covariances used for model estimation in SSM.

of the impulse response matrix (24). Here and in the following the modified cross-spectral density matrix (20) is used. As seen both functions are almost symmetric with time. Definitely, they do not possess any causality. An AR model of order $\acute{p} = 30$ is calibrated with the 2SLS method. This model if represented in a canonical state space form, or Markovian representation [14], corresponds to a state space model of order 900 for the present case. Figure 7 shows time series simulated using the calibrated AR model. The black solid line shows the spatial mean value of the simulated turbulence components. The gray dots show overlaid realizations of the turbulence processes on different nodes of the field.

Next the SSM method is used to estimate a state space model for the turbulence field. Figure 8 shows $\ln(s_i+1)$ where s_i denotes i^{th} singular value, versus singular value number, i, of the block Toeplits matrix $\mathbf{T}$. As can be seen about 120 singular values are considerably larger than the others. This inculcates that the optimum system order is approximately 120 in this case. Figure 9 shows the simulated time series of turbulence using a state space model of order 120. In order to provide a common framework for comparing results of different methods, the same white noise realization is used for simulation with both of the algorithms stated in this example. In what follows plots of auto- and cross-covariance functions are only indicated for positive time separation due to their symmetry property, $\mathbf{C_{vv}}(\tau) = \mathbf{C}^{\mathrm{T}}_{\mathbf{vv}}(-\tau)$.

Figure 10 shows auto-covariance functions of the state space model and the AR model at node 1. Figure 11 shows cross-covariance function of the state space model between nodes 1

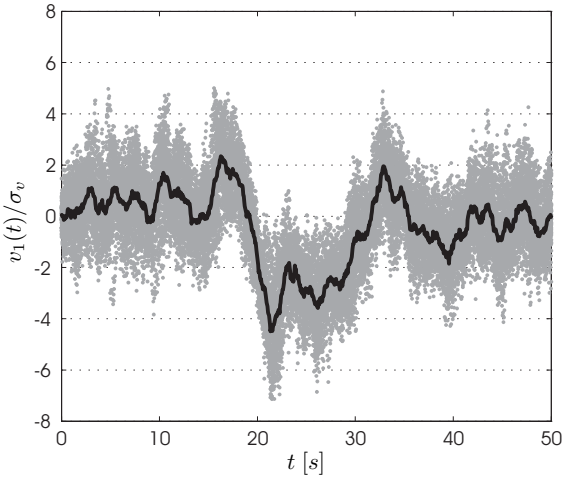

Fig. 9: Numerical simulation of turbulence field based on SSM model, Eq. (32). —: Spatial mean of the turbulence realizations. ·: Spatial distribution of the turbulence realizations.

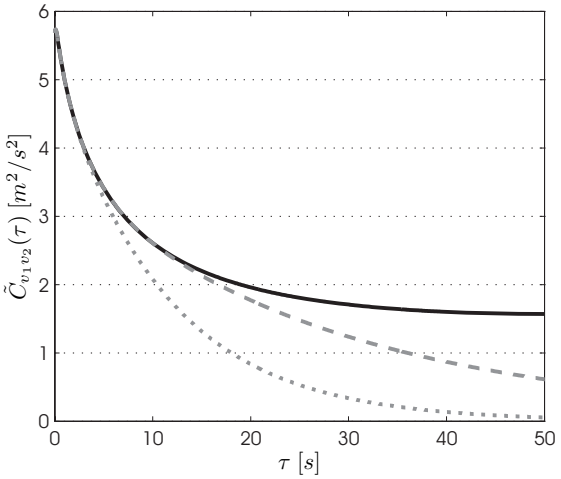

Fig. 11: Cross-covariance functions of the AR and SSM models for vector turbulence between nodes 1 and 2. ——: Covariance matrix, Eq. (13). ..... : 2SLS, Eq.(27). – – –: SSM, Eq.(37).

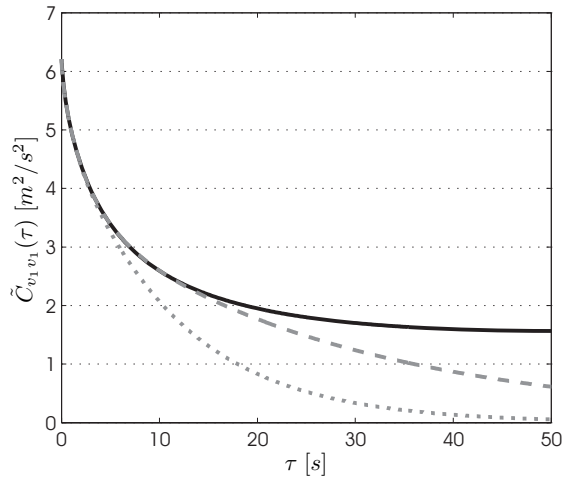

Fig. 10: Auto-covariance functions of the AR and SSM models for vector turbulence at node 1. ——: Covariance matrix, Eq. (13). ..... : 2SLS, Eq.(27). – – –: SSM, Eq.(37).

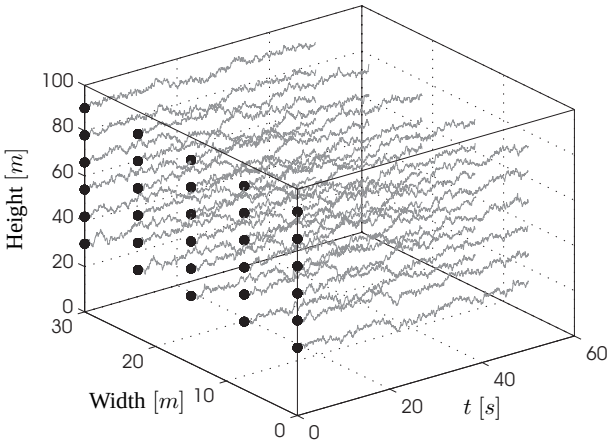

Fig. 12: Simulated turbulence field using SSM

and 2 compared to the theoretical cross-covariance function. As seen the cross-covariance functions of the SSM are in better agreement with the theoretical cross-covariance function than the cross-covariance functions of the AR model of 2SLS. Figure 12 shows the three dimensional representation of the simulated turbulence field generated by the SSM model.

The last context investigated in this research work is the analysis of stability of the calibrated models which is of paramount importance. As explained in the paper, the stability of the state space model might be investigated by examining the magnitude of the eigenvalues of its $\mathbf{A}$ matrix. The magnitude of all of the eigenvalues of a stable discrete state space model must be less than one i.e. all eigenvalues are located in the unit circle in the complex plane. The same criterion is valid about poles of the AR model of the 2SLS i.e. $\mid \lambda^{\acute{p}}\mathbf{I} + \Sigma_{l=1}^{\acute{p}} \lambda^{\acute{p}-l}\mathbf{A}_l \mid = 0$. Therefore magnitudes of all of the poles of the AR model must be less than one. In this regard, Figure 13 shows poles of the AR model of the 2SLS method, whereas figure 14 shows the eigenvalues (poles) of the SSM model. It is seen via the plots that the two methods introduce very different patterns for placement of the poles of their models. Next, figure 15 shows stability of four different models with various model orders for the SSM method. It is seen that increasing order causes instability of the model, c.f. figure 15 for the model order 850. Consequently an upper limit for the model order for the SSM method seems to exist.

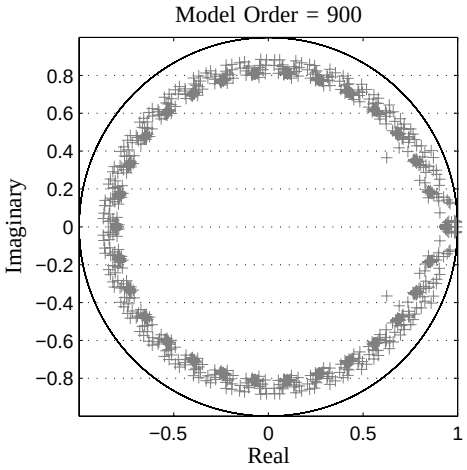

Fig. 13: Poles of the 2SLS model.

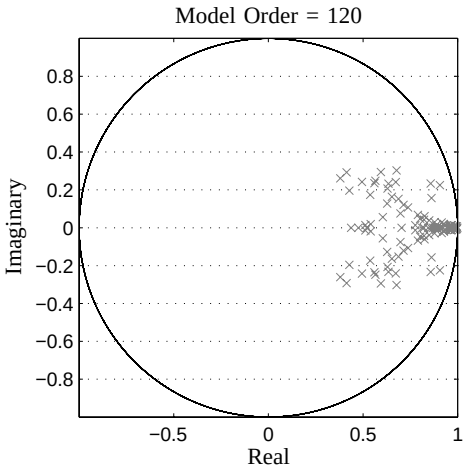

Fig. 14: Poles of the SSM model.

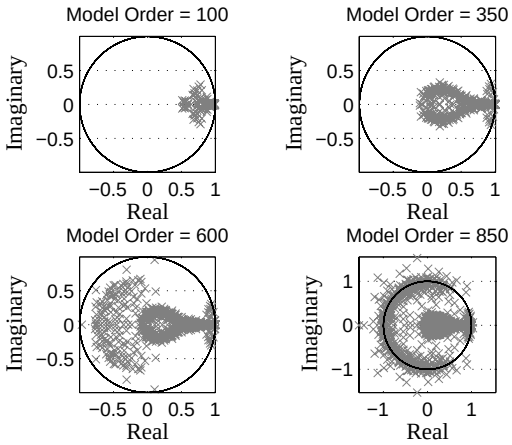

Fig. 15: Poles of the SSM model for various model orders.

VII. Conclusions

The paper addresses calibrating a state space model capable of simulating vector turbulence process incorporating phase spectrum. The Hermitian cross-spectral density matrices representing the spatially discretized turbulence field turn out not to satisfy the positive definiteness condition, mainly in low frequency range. In order to circumvent these problems, two modification schemes based on a Gauss and an eigenvalue decomposition of the cross-spectral density matrix are investigated that guarantee positive definiteness of the modified cross-spectral density matrices. In the paper the SSM method for state space modelling of the vector turbulence process is explained which seems to be a considerably strong method in accurate modelling of the turbulence process. A privilege of the method is that it incorporates a criterion which is very useful in determination of the optimum model order. Analysis of the stability of the models for both the AR model of the 2SLS method and the SSM model reveals that stability proposes an upper band for the model order in SSM method.

VIII. Acknowledgement

The Danish Energy Authority is acknowledged for support under the grant EFP07-II, Estimation of Extreme Responses and Failure Probability of Wind Turbines under Normal Operation by Controlled Monte Carlo Simulation.

References

[1] M. Shinozuka and C.M. Jan, *Digital Simulation of Random Processes and its Applications*. Journal of Sound and Vibration, 25(1), 111-128, 1972.

[2] G. Solari and F.Tubino, *A turbulence Model based on Principal Components*. Probabilistic Engineering Mechanics, 17, 327-335, 2002.

[3] A. Kareem, *Numerical simulation of wind effects: A probabilistic perspective*. Journal of Wind Engineering and Industrial Aerodynamics, 96, 1472-1497, 2008.

[4] X. Chen,A. Kareem, *Aeroelastic analysis of bridges under multi-correlated winds: integrated state-space approach*. Journal of Engineering Mechanics ASCE, 127 (11), 1124-1134, 2001.

[5] J.C. Kaimal, J.C. Wyngaard and Y. Izumi, O.R. Cote, *Spectral Characteristics of Surface-Layer Turbulence*. Quarterly Journal of the Royal Meteorological Society, 98, 1972.

[6] M. Shiotani and Y. Iwayani, *Correlation of Wind Velocities in Relation to the Gust Loadings*. Proceedings of the 3rd Conference on Wind Effects on Buildings and Structures, Tokyo, 1971.

[7] E. Samaras, M. Shinozuka and A. Tsurui, *ARMA representation of random processes*. Journal of Engineering Mechanics ASCE, 111(3), 449461, 1985.

[8] A. Papoulis, *Probability, Random Variables and Stochastic Processes*, 2nd Ed. Mc Graw-Hill, 1984.

[9] W. Gersch and J. Yonemoto, *Synthesis of multivariate random vibration systems: A two-stage least squares AR-MA model approach*. Journal of Sound and Vibration, 52(4), 553-565, 1977.

[10] Y. Li and A. Kareem, *ARMA systems in wind engineering*. Probabilistic Engineering Mechanics, 5(2), 50-59, 1990.

[11] P. Van Overschee and B. De Moor, *Subspace Identification for Linear Systems: Theory-Implementation-Applications*, Dordrecht, Netherlands: Kluwer Academic Publishers, 1996.

[12] H. Akaik, *Stochastic theory of minimal realization*, IEEE Transactions on Automatic Control 19, 667-674, 1974.

[13] T. Katayama, Subspace Methods for System Identification, first ed., Springer, 2005.

[14] H. Akaik, Markovian representation of stochastic processes and its application to the analysis of autoregressive moving-average processes, Annals of the Institute of Statistical Mathematics 26(1), 363-387, 1974.